THE JOURNAL OF PHYSICAL CHEMISTRY A

ARTICLE

pubs.acs.org/JPCA

Ab Inito Study on Triplet Excitation Energy Transfer in Photosynthetic Light-Harvesting Complexes

Zhi-Qiang You[†,‡,§] and Chao-Ping Hsu*[,‡]

[†]Taiwan International Graduate Program and [‡]Institute of Chemistry, Academia Sinica, 128 Section 2 Academia Road, Nankang, Taipei 11529, Taiwan

[§]Department of Chemistry, National Tsing Hua University, 101 Section 2 Kuang-Fu Road, Hsinchu 30031, Taiwan

Supporting Information

ABSTRACT: We have studied the triplet energy transfer (TET) for photosynthetic light-harvesting complexes, the bacterial light-harvesting complex II (LH2) of *Rhodospirillum molischianum* and *Rhodopseudomonas acidophila*, and the peridinin−chlorophyll *a* protein (PCP) from *Amphidinium carterae*. The electronic coupling factor was calculated with the recently developed fragment spin difference scheme (You and Hsu, *J. Chem. Phys.* **2010**, *133*, 074105), which is a general computational scheme that yields the overall coupling under the Hamiltonian employed. The TET rates were estimated based on the couplings obtained. For all light-harvesting complexes studied, there exist nanosecond triplet energy transfer from the chlorophylls to the carotenoids. This result supports a direct triplet quenching mechanism for the photoprotection function of carotenoids. The TET rates are similar for a broad range of carotenoid triplet state energy, which implies a general and robust TET quenching role for carotenoids in photosynthesis. This result is also consistent with the weak dependence of TET kinetics on the type or the number of π conjugation lengths in the carotenoids and their analogues reported in the literature. We have also explored the possibility of forming triplet excitons in these complexes. In B850 of LH2 or the peridinin cluster in PCP, it is unlikely to have triplet exciton since the energy differences of any two neighboring molecules are likely to be much larger than their TET couplings. Our results provide theoretical limits to the possible photophysics in the light-harvesting complexes.

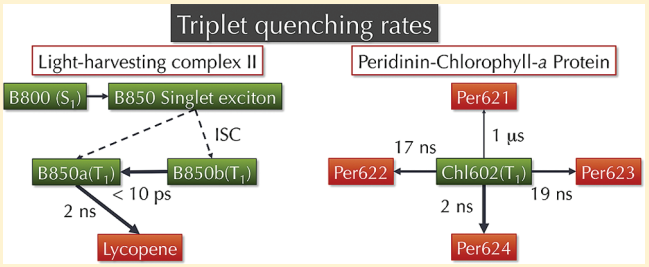

INTRODUCTION

The triplet excitation energy of one molecule or fragment may transfer to a different molecule or fragment via the triplet energy transfer (TET). When a molecule is excited to a singlet excited state, it may undergo intersystem crossing (ISC) to reach a triplet state, and TET may take place. In photosynthesis, part of the excitation in chlorophylls (Chl) or bacteriochlorophylls (BChl) can go through ISC and reach triplet states. Triplet chlorophylls may sensitize the oxygen molecules and generate reactive singlet oxygen which can damage nearby molecules. Carotenoids in photosynthetic complexes can directly quench triplet BChls through the TET process, and avoid the formation of reactive singlet oxygen.[1−5]

Computational studies of TET in photosynthesis have been rare. Early works employed a direct calculation of the exchange integrals to estimate the TET couplings.[6−8] However, the estimated TET rates from the resulting coupling strengths are not consistent with experimental results. Nagae et al.[6] have estimated the transfer matrix elements, and they are between 0.27 and 0.87 meV in several artificial configurations for neurosporene and BChl-*a*. The largest exchange coupling was reported as 0.012 meV in the bacterial light-harvesting complex, LH2 of *Rhodospirillum (Rs.) molischianum*.[7] This coupling value implies a submicrosecond TET time scale, which is much slower than the observed nanosecond kinetics.[5,9] For the peridinin−chlorophyll *a* protein (PCP) of *Amphidinium carterae*, the largest two couplings were reported as 0.593 and 0.037 meV for peridinins Per613 and Per614, respectively.[8] This result does not agree with recent observation from time-resolved electron paramagnetic resonance (TR-EPR) experiments, which concluded that Per614 is major triplet acceptor.[10]

The early works on TET coupling in photosynthetic light-harvesting systems are often based on empirical quantum chemistry models. Semiempirical quantum models are not suitable for TET couplings, since the exponential attenuation of wave functions is implicitly parametrized without a chance of being varied. Many multicentered two-electron integrals were often ignored in empirical models, and they are expected to contribute to the exchange coupling. These restrictions can severely affect the quality of TET coupling, because the TET

Special Issue: Graham R. Fleming Festschrift

Received: January 7, 2011
Revised: February 28, 2011
Published: March 16, 2011

coupling is mainly the Dexter's exchange interaction,[11] a two-electron integral of exchange type, and it involves the overlap of molecular orbitals from the two fragments.[12−15] As a result, TET coupling is a generally small electronic interaction that is mainly due to the interaction of the wave functions in the peripheral region. In a recent work, TET couplings derived from the energy gaps of a semiempirical model, ZINDO, were reported to be about half of those from ab initio Hamiltonians.[16] Therefore, it is interesting to see how a full account of the TET coupling in an ab initio framework would work, since it does not restrict the exponential attenuation of wave functions nor does it skip two-electron integrals of any type.

Recently we have developed the fragment spin difference (FSD) scheme to calculate TET couplings.[15] In our tests for small molecules, the FSD scheme provides the full TET coupling, and it is applicable to general systems with few restrictions. Moreover, the coupling values for small π-conjugating molecules are in the range where nanosecond or even faster TET rates are possible. Therefore, it would be interesting to test the FSD scheme on photosynthetic light-harvesting complexes and gain insights to the possible quenching processes of triplet states.

Carotenoids have been regarded as the quencher for Chl-*a* (or BChl-*a*) triplet state, and one of the possible mechanisms is a direct TET.[5,9,10,17−19] However in the literature a triplet−triplet annihilation mechanism was also proposed and discussed, which involves an interaction of a triplet BChl-*a* and a triplet carotenoid.[20−23] Using purple bacteria strains that lack carotenoids, Monger et al. found that the BChl-*a* triplet states are formed within a few nanoseconds and last over a few tens of microseconds after excited by light.[24] On the other hand, if carotenoid-containing antenna complexes are excited, BChl-*a* triplets are quenched in 20−30 ns[3] and carotenoids triplets are formed in identical kinetics.[9] However, in other works, both carotenoid and BChl-*a* triplets were observed within 10 ps after photoexcitation of BChl-*a*. Both triplet states decay within a few nanoseconds, and therefore the triplet−triplet annihilation mechanism was proposed.[20,21]

The peridinin−chlorophyll protein (PCP) is a soluble light-harvesting protein from dinoflagellates. Peridinin (Per) is a unique carotenoid with eight conjugated double bonds, which is shorter than most carotenoids in light-harvesting complexes, typically with 9−13 conjugated double bonds. In addition, peridinin contains a polar and symmetry-breaking lactone group in its polyene backbone, which can lead to unusual spectroscopic properties.[25] For example, the S_1 state lifetime is known to be strongly dependent on solvent polarity, and a charge-transfer state character was suggested.[26,27] Computational work had also pointed out such a possibility.[28] The light-harvesting and triplet quenching processes have been studied for PCP of *A. carterae* and *Heterocapsa pygmaea*.[10,18,19,22,23,29,30] The triplet peridinin was observed in 17 ns after excitation.[18] It was suggested that triplet Chl-*a* is quenched directly by peridinin via TET. However, the triplet−triplet annihilation was also proposed as a parallel mechanism for triplet Chl-*a* quenching, in order to explain the coexistence of triplet peridinin and Chl-*a* observed in FTIR spectroscopy.[22,23] The crystal structure of PCP from *A. carterae* has been available,[31] and therefore it is also an ideal candidate to test computational predictions.

Computational characterization of TET couplings offers important parameters for the TET rates, and therefore the plausibility of different models can be addressed. In the present work, we report ab initio characterization of TET couplings for three different light-harvesting complexes based on their crystal strucutres,[31−33] and discuss the possible consequences in the light of our results.

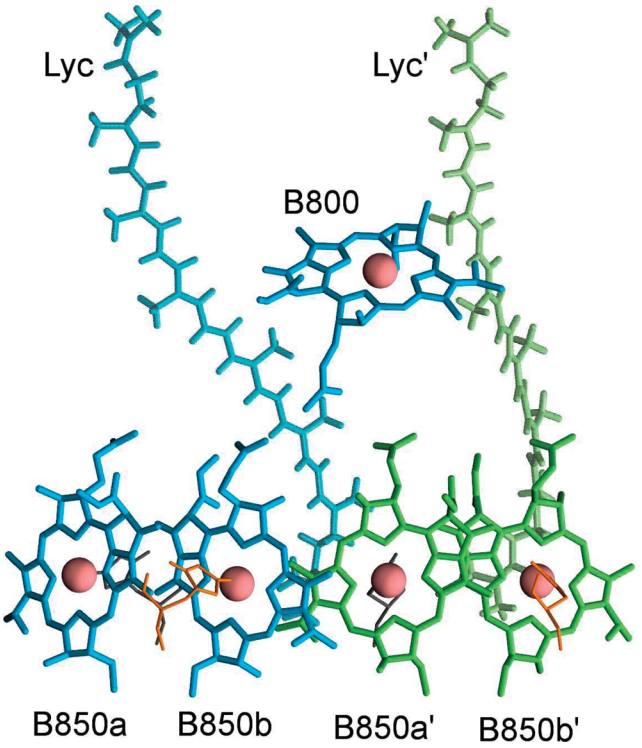

Figure 1. The arrangement of lycopenes and BChl-*a*'s in two adjacent $\alpha\beta$ subunits of the LH2 complex of *Rs. molischianum*.[32] Molecules in the same color are associated with the same $\alpha\beta$-subunit. The histidines coordinating to the magnesium ions in B850 are shown in black and orange. The phytol tails of BChl-*a*'s were removed for clarity.

THEORY AND METHODS

Structure of Light-Harvesting Complex II. The X-ray crystal structure of the LH2 complex from *Rs. molischianum* was reported by Koepke et al.[32] This LH2 is an octamer in an 8-fold symmetric structure. Each subunit is a heterodimer which consists of an α- and a β-apoprotein. Each $\alpha\beta$ subunit contains three BChl-*a* molecules and one lycopene (Lyc) molecule. Two of the BChl-*a*'s are in the B850 complex, which forms singlet excitons, and the third BChl-*a* is in the B800 complex. The arrangement of BChl-*a*'s and lycopenes within two adjacent $\alpha\beta$-subunits is depicted in the Figure 1.

Since the electronic coupling of TET is basically an exchange interaction, close contact is necessary for a significant value. Therefore, we chose the lycopene and its neighboring BChls for TET study. The B850 complex forms an energy trap in the LH2,[34] and it is the potential site for triplet state formation.[3] The lycopene is in close contact with one BChl-*a* within the same $\alpha\beta$-subunit (labeled as B850b in Figure 1) and another BChl-*a* on the adjacent subunit (labeled as B850a′), and both cases were studied in the present work. In order to investigate possible role of B800 molecules in the triplet quenching, we have also picked a B800-Lyc′ pair. In spired by the interesting excitonic effects arising from a weak coupling in the B800 in the *singlet* state,[35] we have studied the possibility of B850 *triplet* exciton formation in the present work, by calculating the TET coupling for neighboring dimers in B850.

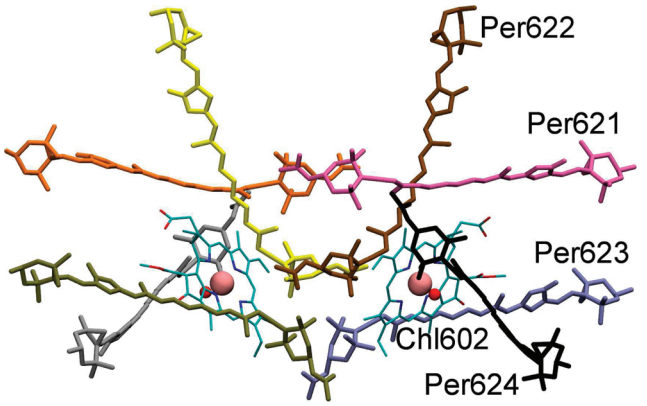

Figure 2. The arrangement of peridinins and Chl-*a*'s in a PCP monomer.[31] The oxygen atoms of the water molecules are shown as red spheres.

The structure of the LH2 complex from *Rhodopseudomonas (Rps.) acidophila* is also available from the literature.[33,36,37] The structure is roughly similar to that of *Rs. molischianum* but with a nonameric ring assembly. The carotenoid rhodopin glucoside (RG) is in the place of lycopene. The molecular pairs picked for the present study are the same as those for *Rs. molischianum*, since the molecules are arranged similarly to those shown in Figure 1.

Structure of Peridinin−Chlorophyll *a* Protein. The peridinin−chlorophyll *a* protein (PCP) of *A. carterae* is a trimeric complex, and each monomeric PCP unit has two structurally similar domains.[31] Each domain includes a Chl-*a* and four peridinin molecules. The arrangement of the pigment clusters in the PCP is depicted in Figure 2. Each of the four peridinins in the cluster is potentially capable of quenching chlorophyll triplet since the π-conjugated regions of all four peridinins are in van der Waals contact to the tetrapyrrole ring of the Chl-*a*, with distances of 3.3−3.8 Å.[31] So all four peridinin−Chl-*a* pairs are included in the present study. In addition, it may be possible to have delocalized triplet states in the peridinin cluster,[38] and this may affect the quenching dynamics. Therefore, we have also calculated the TET couplings between two peridinins in the cluster. A water molecule is seen between Chl602 and Per624 (also seen between Chl601 and Per614) in the crystal structure, and we test for its effect on TET coupling.

Triplet Energy Transfer Rate. TET involves a change in the electronic configuration. In the weak-coupling limit, the rate for TET can be described by Fermi's golden rule[39]

$$k_{\mathrm{TET}} = \frac{2\pi}{\hbar}|H_{\mathrm{if}}|^2\delta(E_{\mathrm{i}} - E_{\mathrm{f}}) \tag{1}$$

In eq 1, H_{if} is the electronic coupling between two electronic states, $|\mathrm{i}\rangle$ and $|\mathrm{f}\rangle$ where the triplet excitation is on the donor and the acceptor, respectively. The δ function is for energy conservation in the transition. For most systems of interest, it is necessary to consider a dense collection of states, and thus a Franck−Condon weighted density of states (FCWD) is often used.[40] In singlet energy transfer, the Förster theory[41] uses an overlap integral of donor emission and acceptor absorption spectra, which provides both the transition dipole strengths and the FCWD. A similar approach for TET rate that uses spectra to estimate FCWD is developed in the literature[11,40] and it is outlined below.

The transition probability of a system, starting with an electronic state i and ends with state f can be written as[40]

$$k_{\mathrm{if}} = \frac{2\pi}{\hbar}\sum_{\mu}\sum_{\nu} p(\varepsilon_{\mathrm{i}\mu})|\langle\Theta_{\mathrm{i}\mu}|H_{\mathrm{if}}|\Theta_{\mathrm{f}\nu}\rangle|^2\delta(\varepsilon_{\mathrm{i}\mu} - \varepsilon_{\mathrm{f}\nu}) \tag{2}$$

where $p(\varepsilon_{\mathrm{i}\mu})$ is the Boltzmann population of the state i and vibration level μ. $\varepsilon_{\mathrm{i}\mu}$ (or $\varepsilon_{\mathrm{f}\nu}$) is the vibronic energy, and $\Theta_{\mathrm{i}\mu}$ (or $\Theta_{\mathrm{f}\nu}$) is the vibrational wave function, for electronic state i (or f) and vibration state μ (or ν) for the full system. Under the Condon approximation, and assuming independent nuclear motion in the donor and acceptor, we can separate the donor and acceptor states, and rewrite eq 2 as[40]

$$k_{\mathrm{if}} = \frac{2\pi}{\hbar}\left|H_{\mathrm{if}}\right|^2 \sum_{\mu,\nu\,\in\,\mathrm{D}}\ \sum_{\mu',\nu'\,\in\,\mathrm{A}} p(E^{\mathrm{D}}_{\mathrm{i}\mu})p(E^{\mathrm{A}}_{\mathrm{i}\mu'})|\langle\theta^{\mathrm{D}}_{\mathrm{i}\mu}|\theta^{\mathrm{D}}_{\mathrm{f}\nu}\rangle\langle\theta^{\mathrm{A}}_{\mathrm{i}\mu'}|\theta^{\mathrm{A}}_{\mathrm{f}\nu'}\rangle|^2 \times \delta(\Delta E^{\mathrm{D}}_{\mathrm{f}\nu,\mathrm{i}\mu} + \Delta E^{\mathrm{A}}_{\mathrm{f}\nu',\mathrm{i}\mu'}) \tag{3}$$

where $\Delta E^{\mathrm{D(A)}}_{\mathrm{f}\nu,\mathrm{i}\mu} = E^{\mathrm{D(A)}}_{\mathrm{f}\nu} - E^{\mathrm{D(A)}}_{\mathrm{i}\mu}$ is the difference in vibronic energy for the donor (or acceptor) from the initial to the final state. In the derivation of eq 3, the state energies ($\varepsilon_{\mathrm{i}\mu}$ and $\varepsilon_{\mathrm{f}\nu}$) are assumed to be the sum of the donor and acceptor energies in their corresponding vibronic states

$$\varepsilon_{\mathrm{i}\mu} = E^{\mathrm{D}}_{\mathrm{i}\mu} + E^{\mathrm{A}}_{\mathrm{i}\mu'} \tag{4}$$

and a similar definition is used for $E^{\mathrm{D(A)}}_{\mathrm{f}\nu(\nu')}$. $\theta^{\mathrm{D(A)}}_{\mathrm{i}\mu}$ are vibration wave functions for one of the fragments in the corresponding electronic state. The transition rate k_{if} in eq 3 can be rewritten by separating terms for the donor and the acceptor and using the following expressions

$$f_{\mathrm{D}}(E) = \sum_{\mu}\sum_{\nu} p(E^{\mathrm{D}}_{\mathrm{i}\mu})|\langle\theta^{\mathrm{D}}_{\mathrm{i}\mu}|\theta^{\mathrm{D}}_{\mathrm{f}\nu}\rangle|^2\delta(E + \Delta E^{\mathrm{D}}_{\mathrm{f}\nu,\mathrm{i}\mu}) \tag{5}$$

$$f_{\mathrm{A}}(E) = \sum_{\mu'}\sum_{\nu'} p(E^{\mathrm{A}}_{\mathrm{i}\mu'})|\langle\theta^{\mathrm{A}}_{\mathrm{i}\mu'}|\theta^{\mathrm{A}}_{\mathrm{f}\nu'}\rangle|^2\delta(E - \Delta E^{\mathrm{A}}_{\mathrm{f}\nu',\mathrm{i}\mu'}) \tag{6}$$

which are density of states weighted by vibrational Franck−Condon factors, or the FCWD functions. With the FCWD functions, k_{if} as in eq 3 is now

$$k_{\mathrm{if}} = \frac{2\pi}{\hbar}|H_{\mathrm{if}}|^2\int_{-\infty}^{\infty} \mathrm{d}E f_{\mathrm{D}}(E)f_{\mathrm{A}}(E) \tag{7}$$

It is possible to use experimental optical spectra for the FCWD functions. For example, the absorption cross section for the acceptor is used[42]

$$\sigma^{\mathrm{A}}_{\mathrm{if}}(\omega) = \left[\frac{n}{\varepsilon}\left(\frac{\mathcal{E}_{\mathrm{e}}}{\mathcal{E}}\right)^2\right]\frac{4\pi^2\omega}{3\hbar c}\left|\mathbf{M}^{\mathrm{A}}_{\mathrm{if}}\right|^2\sum_{\mu'}\sum_{\nu'} p(\omega^{\mathrm{A}}_{\mathrm{i}\mu'})|\langle\theta^{\mathrm{A}}_{\mathrm{i}\mu'}|\theta^{\mathrm{A}}_{\mathrm{f}\nu'}\rangle|^2 \times \delta(\omega - \omega^{\mathrm{A}}_{\mathrm{f}\nu',\mathrm{i}\mu'}) \tag{8}$$

and the transition probability of spontaneous emission, for the donor is

$$A^{\mathrm{D}}_{\mathrm{if}}(\omega) = \left[\frac{n^3}{\varepsilon}\left(\frac{\mathcal{E}_{\mathrm{e}}}{\mathcal{E}}\right)^2\right]\frac{4\omega^3}{3\hbar c^3}\left|\mathbf{M}^{\mathrm{D}}_{\mathrm{if}}\right|^2\sum_{\mu}\sum_{\nu} p(\omega^{\mathrm{D}}_{\mathrm{i}\mu})|\langle\theta^{D}_{\mathrm{i}\mu}|\theta^{\mathrm{D}}_{\mathrm{f}\nu}\rangle|^2 \times \delta(\omega + \omega^{\mathrm{D}}_{\mathrm{f}\nu,\mathrm{i}\mu}) \tag{9}$$

In both eqs 8 and 9, $\mathbf{M}_{\mathrm{if}}$ is the transition moment, which is a dipole matrix element for singlet spectra. For transitions between a singlet and a triplet state, $\mathbf{M}$ should include the spin−orbit coupling

operator. The factors in the square brackets of eqs 8 and 9 are corrections for electric fields for molecules in a medium:[43] n and ε are the refractive index and dielectric constant of the medium, respectively, and $\mathcal{E}_e$ is the effective electric field for the electrons inside a media, which may be different from the averaged field $\mathcal{E}$.

We now have the FCWD functions expressed as

$$f_A(E) = \frac{\sigma_{if}^A(E)/E}{\int_{-\infty}^{\infty} dE \sigma_{if}^A(E)/E} \quad (10)$$

and

$$f_D(E) = \frac{A_{if}^D(E)/E^3}{\int_{-\infty}^{\infty} dE A_{if}^D(E)/E^3} \quad (11)$$

in which we have used the relationship[42]

$$\sum_{\mu}\sum_{\nu} p(\omega_{i\mu}^{D(A)})|\langle\theta_{i\mu}^{D(A)}|\theta_{f\nu}^{D(A)}\rangle|^2 = 1 \quad (12)$$

Therefore, the rate in eq 1 can be expressed by[11]

$$k_{TET} = \frac{2\pi}{\hbar}|H_{if}|^2 J \quad (13)$$

where J is the overlap integral of the FCWD functions,

$$J = \int_{-\infty}^{\infty} dE f_D(E) f_A(E) \quad (14)$$

The FCWD functions and subsequently J were calculated using experimental spectra, which were fitted using the following expressions[44,45]

$$A_{if}^D(E) = \sum_{m=0}^{\infty}\left(\frac{E_0 - m\hbar\omega}{E_0}\right)^3\left(\frac{S^m}{m!}\right)\exp\left[-4\ln 2\left(\frac{E - E_0 + m\hbar\omega}{\text{fwhm}}\right)^2\right] \quad (15)$$

$$\sigma_{if}^A(E) = \sum_{m=0}^{\infty}\left(\frac{E_0 + m\hbar\omega}{E_0}\right)\left(\frac{S^m}{m!}\right)\exp\left[-4\ln 2\left(\frac{E - E_0 - m\hbar\omega}{\text{fwhm}}\right)^2\right] \quad (16)$$

where E_0 is the 0−0 transition energy and $\hbar\omega$ denotes the energy of a vibration quanta. S is the Huang−Rhys factor,[46] which is a dimensionless measurement for the displacement of the equilibrium structures in the ground and excited states. In this approach, it is assumed that only one vibration mode is heavily coupled to the excitation. The vibronic bands are broadened to account for effects of all other modes and solvent effects, with its full width at half-maximum denoted as "fwhm". We note that expressions in eqs 15 and 16 have been useful for analyzing spectra for transition-metal complexes[45] and in the calculation of singlet energy transfer rates.[47−49] With fitted parameters, we simulated the FCWD functions as given in eqs 10 and 11, and calculated the FCWD overlap, J, as in eq 14.

We note that the triplet spectra are not always available in the literature, especially for the carotenoids. It was reported that the vibronic features of the T_1 spectrum for octatetraene are very similar to the S_1 and S_2 spectra.[50] Thus, we have used the S_2 spectra in the place of triplet spectral line shapes for the carotenoids. The 0−0 transition energy for the T_1 state of the carotenoids is unknown. Following an empirically observed trend for polyenes reported in the literature,[50,51] we have used half of S_1 state energy of the carotenoids as an estimate for the T_1 state. We have also scanned over a range of this value to see its influence on the TET rates.

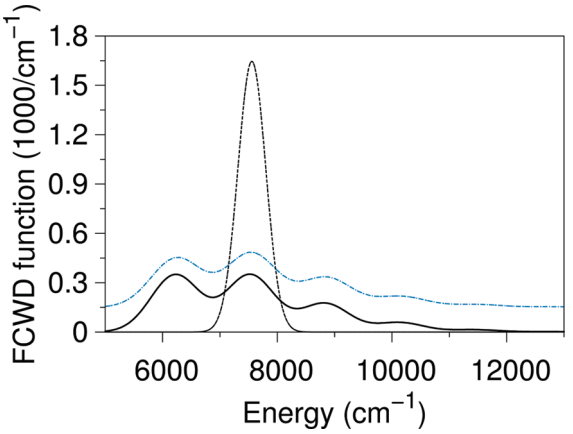

Figure 3. The FCWD functions for BChl-*a* (dashed line), lycopene (black solid line), and RG (blue dashed-dotted line, shifted up by 0.15) calculated with eqs 10 and 11 and with parametrized spectra eqs 15 and 16. For BChl-*a*, the pararmeters S and fwhm used are 0 and 570 cm^{-1}, respectively, with E_0 as 7580 cm^{-1}. For lycopene, the parameters S, $\hbar\omega$, and fwhm of the vibronic bands are 1.0, 1300 cm^{-1}, and 993 cm^{-1}, respectively. E_0 was estimated as 6250 cm^{-1}.[53] For RG, the parameters S, $\hbar\omega$, and fwhm are 1.1, 1300 cm^{-1}, and 1040 cm^{-1}, respectively. E_0 was estimated to be 6280 cm^{-1}.[54] For both carotenoids, the number of vibronic bands was truncated to eight as the progression converges.

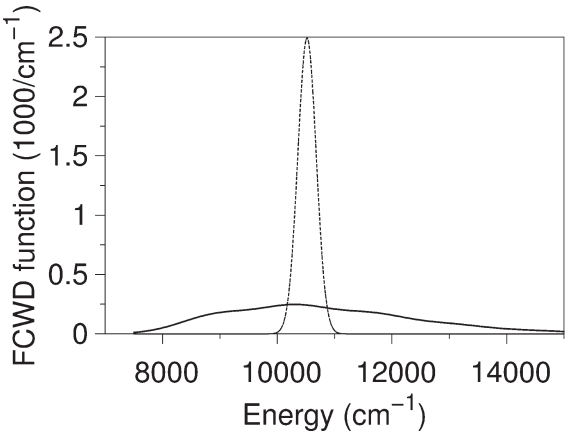

Figure 4. The FCWD functions for Chl-*a* (dashed line) and peridinin (solid line) calculated with eqs 10 and 11 and with parametrized spectra eqs 15 and 16 For Chl-*a*, the parameters S and fwhm are 0 and 377 cm^{-1}, respectively, with E_0 as 10500 cm^{-1}.[55] For peridinin, the parameters S, $\hbar\omega$, and fwhm are 1.4, 1350 cm^{-1}, and 1500 cm^{-1}, respectively. E_0 was estimated to be 9000 cm^{-1}.[25] The number of vibronic bands was truncated to eight as the progression converges.

In an LH2 complex, BChl-*a* can transfer the triplet energy to the carotenoid or to another BChl-*a*. Phosphorescence spectrum of BChl-*a* in LH2 is available in the literature[21] and it was used directly as the donor emission spectrum. The triplet absorption spectrum was assumed to be the mirror image of the phosphorescence. The Stokes shift of the triplet spectra was assumed to be the same as that of the singlet spectra. In other words, the peak difference of ^1Q_y absorption and emission bands of BChl-*a* was used to model the peak position of triplet absorption spectrum.[21]

We can barely find any triplet spectrum for lycopene. We took the spectra of S_2 absorption for the line shape.[52] The 0−0 transition for T_1, E_0, is then scanned over a range to see the possible TET rates. We also took half of the S_1 energy for an estimated E_0 for T_1, which is 6250 cm^{-1}.[53] This is a value derived from lycopene in *n*-hexane, and it is believed to be an upper limit for lycopene in the LH2 complex.

For the carotenoid RG in the LH2 complex of *Rps. acidophila*, the triplet spectrum is similarly estimated using the S_2 absorption for the line shape.[54] Again E_0 of the T_1 state was estimated from half of the S_1 state energy, which is 6280 cm^{-1}.[54]

For TET in PCP, Chl-*a* is the triplet energy donor and peridinin, the acceptor. Chl-*a* T_1 emission peak position is reported in the literature.[55] The singlet fluorescence spectrum was used to mimic the triplet spectral line shape.[56] Like lycopene and RG, peridinin does not have much triplet spectral data available in the literature. We took best fit of the line shape for the S_2 absorption spectrum,[57] and tuned the E_0 for simulating TET reaction rate. The E_0 for peridinin was estimated as 9000 cm^{-1} from half of the S_1 state energy.[25]

The simulated FCWD functions of donor and acceptor, using eqs 15 and 16, are included in Figure 3 for LH2 and Figure 4 for PCP. The fitted parameter values are included in the captions. From these FCWD functions the *J* overlap factor (eq 7) was obtained in estimating the TET rates.

Electronic Coupling. In a TET process, the initial and final states $|i\rangle$ and $|f\rangle$ are two different spin-localized states. We employed the fragment-spin difference (FSD) scheme[15] to calculate TET coupling. FSD takes two eigenstates, performs a linear combination, and optimizes for the most spin-localized diabatic states from which the off-diagonal Hamiltonian matrix element is calculated. To characterize the extent of spin localization, the spin difference matrix element was defined

$$\Delta s_{mn} = \int_{\mathbf{r}\in \mathrm{D}} \sigma_{mn}(\mathbf{r})\, d\mathbf{r} - \int_{\mathbf{r}\in \mathrm{A}} \sigma_{mn}(\mathbf{r})\, d\mathbf{r} \qquad (17)$$

where $\sigma_{mn}(\mathbf{r})$ is the spin density operator projected to eigenstates $|m\rangle$ and $|n\rangle$, and the integrations are over the donor (D) or acceptor (A) fragment space. Maximizing the difference of diagonal FSD matrix element difference gives rise to a pair of optimal spin-localized states, which are regarded as the diabatic states in TET. The off-diagonal Hamiltonian matrix element in the spin-localized, diabatic state is the transfer matrix element

$$H_{\mathrm{if}} = \frac{(E_m - E_n)\Delta s_{mn}}{\sqrt{(\Delta s_{nn} - \Delta s_{mm})^2 + 4\Delta s_{mn}^2}} \qquad (18)$$

FSD is a generalization from similar schemes in the calculation of electron transfer coupling strengths such as the generalized Mullikan−Hush[58] or the fragment charge difference.[59] It is very similar to the fragment excitation difference scheme developed for singlet energy transfer coupling.[60] Other localization techniques can also be used toward the construction of spin-localized diabatic states, such as the Boys localization.[61]

Other Computational Details. The geometries of all carotenoids and chlorophylls in the present study are obtained from X-ray crystal structures.[31−33] To reduce computational cost, the phytol tails of Chl-*a* and BChl-*a* were removed. Hydrogen atoms were added to cap the broken bonds. We are interested in pairs of molecules in close contact, and therefore, the optimizations for all H atoms were performed in the pairs of molecules in which TET was studied, with the coordinates of heavy atoms fixed. The H atoms were optimized using density functional theory (DFT) with the B3LYP hybrid functional[62−64] and 6-31G** basis sets. The FSD couplings throughout this work were calculated using Hartree−Fock configuration interaction single (HF-CIS) with 6-31+G* basis sets.

Table 1. TET Couplings and Rate Constants for Pairs of Pigment Molecules in LH2 Complex

TET pairs	coupling[a]	k_{TET}[b]	TET lifetime
	Rs. molischianum		
B850a′−Lyc	1.082	4.35×10^8	2.30 ns
B850a′ + His−Lyc	0.8919	2.96×10^8	3.38 ns
B850b−Lyc	0.009738	3.52×10^4	28.4 μs
B850b + His−Lyc	0.01099	4.49×10^4	22.3 μs
B800−Lyc′	0.06708	1.67×10^6	598 ns
B850a−B850b	29.74	1.21×10^{11}	8.25 ps
B850a′−B850b	46.52	2.96×10^{11}	3.37 ps
B850a′ + His−B850b + His	45.34	2.82×10^{11}	3.55 ps
	Rps. acidophila		
B850a′−RG	3.358	4.07×10^9	0.246 ns
B850b−RG	0.03347	4.04×10^5	2.48 μs
B800−RG′	0.2702	2.63×10^7	38.0 ns
B850a−B850b	25.28	8.76×10^{10}	11.4 ps
B850a′−B850b	20.52	5.78×10^{10}	17.3 ps

[a] In units of cm^{-1}. Shown are coupling values between the ^3Q_y state of BChl-*a* and the 1^3B_u state of lycopene. [b] In units of s^{-1}. Rate constants calculated using eq 13. The FCWD overlap J_{DA} employed for BChl-*a* and lycopene pairs is 2.53 eV^{-1} (maximum possible value), for BChl-*a* and RG, 2.46 eV^{-1} (maximum possible value), and for BChl-*a* dimers, 0.93 eV^{-1}.

The electronic states of Chl-*a* and BChl-*a* studied can be affected by molecules nearby. For LH2, there is a histidine (His) as the axial coordinating ligand for every BChl-*a* in B850. We have tested for the effects of His by including it in calculation, and compared the results from the same calculation without His. For PCP, as a water-soluble protein, a water molecule was found between Chl602 and Per624, and another one between Chl601 and Per614, in the crystal structure.[31] It was reported that the water molecule has a significant contribution to intermolecular interaction energy between Chl602 and Per624.[65] This water molecule may mediate the TET coupling as proposed in the literature.[10] We have also tested for the effects of this water molecule on TET couplings.

All ab initio calculations in the present work were performed using a developmental version of Q-Chem quantum chemistry package.[66] Spectral simulation and the FCWD overlaps were calculated using programs written in MATLAB.[67]

RESULTS AND DISCUSSION

TET in LH2. *Electronic Couplings.* In Table 1 we list the TET couplings for pigments in LH2. The electronic coupling of TET is a short-range interaction and requires the wave function overlap of interacting molecules.[11] In our previous work,[15,68] a pair of fully stacked π-conjugated molecules has electronic couplings about 200 cm^{-1} at 4.0 Å separation, which is probably the maximum TET coupling size. With a partial π−π contact, the couplings for BChl-*a*'s in the B850 of LH2 are roughly in the expected order of magnitude in the light of previous TET studies.[68] As seen in Table 1,

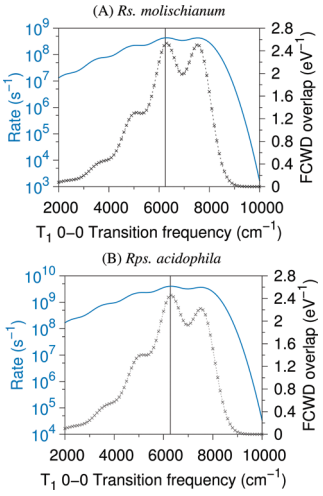

Figure 5. Calculated FCWD overlap integrals (dotted line with crosses, linearly scaled to the right) and TET rate constants (blue solid line, log-scaled to the left), as a function of carotenoid T_1 0−0 transition frequency, for B850a′−Lyc in the LH2 complex of *Rs. molischianum* (A), and for B850a′−RG in the LH2 of *Rps. acidophila* (B). The vertical line indicates the position of the estimated Lyc and RG T_1 0−0 transition frequency, 6250 cm^{-1} and 6280 cm^{-1}, respectively.

the largest TET coupling between BChl-*a* and the carotenoid is with B850a′ in both cases. This result is consistent with the structural characteristic since they have the shortest interpigment distance and the best $\pi-\pi$ contact.[7]

In Table 1 we also list results from calculations with or without the axial His ligand for the BChl-*a* molecules for the LH2 of *Rs. molischianum*. In the three cases studied, it is seen that the inclusion of His may increase or decrease the TET coupling, and in this case the couplings are changed by about 10% or less. Therefore we conclude that the His ligand from the protein does not affect the general size of TET coupling of BChl-*a*.

In the B850 ring of LH2 derived from *Rs. molischianum*, the distance between BChl-*a* is about 3.5−4.0 Å. The $\pi-\pi$ contacts for BChl-*a*'s within the same $\alpha\beta$-subunit are through chlorin ring III, while BChl-*a*'s on neighboring subunits are contacted via their chlorin ring I. The calculated TET couplings between neighboring BChl-*a*'s in B850 are 30 and 47 cm^{-1} for *Rs. molischianum* and 25 and 21 cm^{-1} for *Rps. acidophila* . The large difference in the coupling between B850a′ and B850b is likely from the structure: the distance of the nearest heavy atoms between B850a′ and B850b in *Rps. acidophila* is larger by 0.2 Å. If we assume that the rate of exponential decay with distance is 2.59 Å^{-1} as observed previously,[68] the 0.2 Å difference in distance leads to a factor of exp(−2.59 × 0.2) (≈0.6) in TET coupling, which largely accounts for the discrepancy. We note that 0.2 Å is very close to the structural resolution of the crystal structures. Therefore we discuss our results based on the order of magnitudes of the couplings in the following sections.

TET Rates. In addition to chemically scavenge the singlet oxygen, carotenoids are also known to be able to physically quench the triplet state chlorophylls and therefore prevent formation of singlet oxygen,[1,3,69] which is the model we follow and test in the present work.

TET rate from BChl-*a* to lycopene was calculated using the eq 13. As shown in Figure 5, the maximum FCWD overlap is

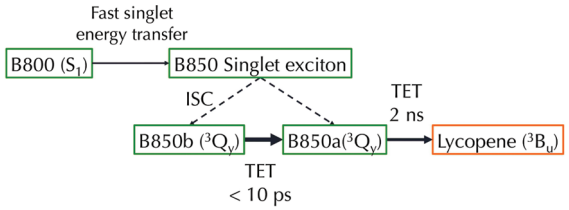

Figure 6. Possible triplet generating and quenching pathways for BChl-*a* and lycopene in LH2.

2.53 eV^{-1} at 6300 cm^{-1} for lycopene T_1 0−0 energy, which is very close to the estimated T_1 energy for lycopene, 6250 cm^{-1}.[53]

The TET kinetics in the LH2 from *Rps. acidophila* could be well-resolved, and the decay kinetics of triplet BChl-*a* was reported to be in the range of 10−26 ns, depending on the temperature.[9] Our calculated TET rates are included in Table 1 and Figure 5. The largest TET coupling with carotenoids is from B850a in the neighboring subunit. The corresponding reaction lifetime is about 2 ns at the maximum FCWD overlap for lycopene and 0.2 ns for RG. Our calculated TET rates are faster, but still largely consistent with the observed TET kinetics in LH2.[9]

From Figure 5, we note that there is a broad range of T_1 energy that gives rise to nanosecond TET. It is mainly due to the large spectral progression in the vibronic bands of both carotenoids. Since the energy levels are likely varied in a protein complex, both dynamically and statically, this result implies the robustness and general applicability of using carotenoids in TET as a quenching mechanism. This result is consistent with an earlier work where TET in LH2 incorporated with two spheroidene analogues with shorter π-conjugations were studied.[70] The triplet quenching efficiencies were similar for both the LH2 incorporated with the 9- and 10-conjugated-double-bond carotenoids, 3,4-dihydrospheroidene, and spheroidene, despite their different T_1 state energies.[70] Another similar result is seen in ref 5, where the TET rates between BChl and carotenoid were reported to be faster than 7 ns, and it is relatively independent of carotenoid type in the different strains of *Rhodopseudomonas sphaeroides* studied. In ref 9, the fastest components in the TET kinetics were reported to vary from 26 to 220 ns (5 K) for LH2 complexes with three different carotenoids (with 9, 10, and 11 conjugated double bonds). Even though the triplet kinetics are "strongly species dependent" as described by the authors, we note that the fastest TET kinetic components are within 1 order of magnitude across the three carotenoids. Therefore, we believe that the prediction of weak dependence on carotenoid energy for TET rate is likely correct.

Triplet Exciton. It was reported that a weak coupling (27 cm^{-1}) in the singlet excitation of B800 complex leads to delocalized excitons, with interesting effects in the spectral line shape and the dynamics of singlet energy transfer.[35] The TET couplings among B850 chromophores are in a similar range, 30−45 cm^{-1}. However, unlike B800, the two B850 molecules within the same $\alpha\beta$-subunit of LH2 (Figure 1) have different structures, which could affect their excitation energies. We have performed time-dependent DFT (TDDFT) calculation to estimate triplet excitation energies of B850 molecules. TDDFT for triplet states is less accurate than that for the singlet states,[71−73] especially for hybrid and range-separated functionals.[71,74] However for molecules with extended π conjugations, an accuracy of 0.2 eV has been reported.[75−77] With the PBE functional[78] and 6-31+G* basis, the TDDFT vertical excitation energies are 0.9344 and 0.8750 eV for B850b and B850a, respectively. In

dx.doi.org/10.1021/jp200200x |J. Phys. Chem. A 2011, 115, 4092–4100

Table 2. TET Coupling and the Maximum Possible TET Rate Constants, between Chl602 and Its Four Neighboring Peridinins in PCP

peridinin	coupling[a]	k_{TET}[b]	TET lifetime (ns)
Per621	0.05219	7.89×10^5	1270
Per622	0.4451	5.74×10^7	17.4
Per623	0.4251	5.24×10^7	19.1
Per623 + W[c]	0.4922	7.02×10^7	14.2
Per624	1.493	6.46×10^8	1.55
Per624 + W[c]	0.9972	2.88×10^8	3.47

[a] In units of cm^{-1}. Listed are TET couplings between the ^3Q_y state of Chl-*a* and the ^3B_u state of peridinin. [b] In units of s^{-1}. Rate constants calculated using eq 13 with the maximum FCWD overlap value, 1.98 eV^{-1}. [c] A bridging water molecule (W55) was included in the calculation.

Table 3. TET Coupling (in units of cm^{-1}) between Peridinins in PCP

	Per623	Per622	Per621
Per624	0.06468	$<10^{-4}$	$<10^{-4}$
Per623		$<10^{-4}$	$<10^{-4}$
Per622			0.3278

other words, the energy difference due to different structure is nearly 500 cm^{-1}, which is more than 10 times larger than the TET coupling. In the light of this computational result, it would be unlikely that the triplet excitations would delocalize to more than one molecule and form excitons. Therefore, we believe that the TET in LH2 is mainly incoherent.

In the light of our computational results, the evolution of triplet excitation in the LH2 from *Rs. molischianum* is depicted in Figure 6. There exists delocalized singlet exciton in B850.[79−81] The excitation can undergo intersystem crossing to form triplet states. The triplet state coherence may rapidly relax due to the large site-energy difference and the relatively weak TET coupling. Thus, the triplet states are likely be localized on B850a and B850b sites. TET can take place from B850b to B850a (or B850a′ in the neighboring subunit) in picoseconds. B850a triplet is then rapidly quenched by a neighboring lycopene in less than 10 ns. The calculated TET rate between B800 and lycopene is less efficient, but with a fast singlet energy transfer from B800 to B850,[82] the chance of forming a triplet BChl-*a* in B800 is low. This way the triplet BChl-*a* is not accumulated and the singlet oxygen conversion was avoided. We note that the process is very similar for the LH2 from *Rps. acidophila* with similar TET couplings (Table 1).

TET in PCP. The calculated TET couplings between Chl-*a* and peridinin in PCP are listed in Tables 2 and 3. As expected, Chl602 and Per624 are known to be in the closest center-to-center distance,[31] and they have the largest TET coupling. For other three pairs, Chl602−Per621 has the smallest coupling value. This may be due to their poor $\pi-\pi$ contact. We note that the bridging water molecule can bring a negative contribution to the TET couplings as seen in the case of Chl602−Per624. This is a case where the water-mediated coupling is opposite in phase to direct through-space coupling. In both cases studied, the TET couplings are within the same order of magnitude when the bridging water molecule is considered.

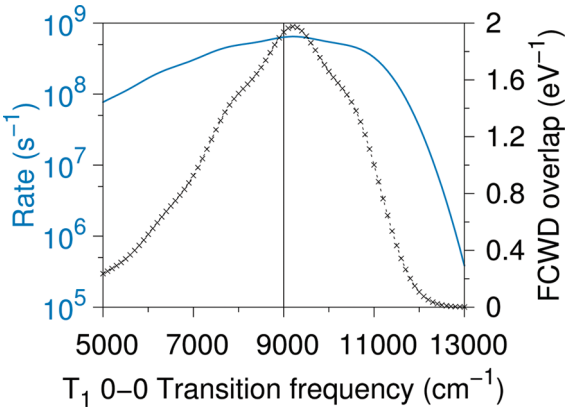

Figure 7. Calculated FCWD overlap integrals (dotted line with crosses, linearly scaled to the right) and TET rate constants (blue solid line, log-scaled to the left) as a function of peridinin T_1 0−0 transition frequency, for TET between Chl602 and Per624 in PCP. The vertical line indicates the corresponding position of the estimated peridinin T_1 0−0 transition frequency (9000 cm^{-1}).

We have calculated TET rates for all Chl-*a* and peridinin pairs using the eq 13. As seen in Figure 7, the maximum FCWD overlap is 1.98 eV^{-1} with peridinin T_1 0−0 energy as 9200 cm^{-1}. This maximum position is also very close to the estimated T_1 energy, 9000 cm^{-1}, which is derived from half of S_1 energy.[25] The resulting TET rates for Chl-*a* and peridinin quenching pathways are listed in Table 2. We can see that the most efficient quenching is through Chl602−Per624 pair, which has a TET time scale of 2 or 4 ns. The minor quenchers to Chl-*a* triplet are Per622 and Per623, with their reaction time scales at about 20 ns. These nanosecond TET time scales are consistent with the observed rising time of peridinin triplet in PCP.[18]

It was reported that peridinin triplets are mainly distributed on Per624 from the results of TR-EPR spectra of photoexcited PCP.[10] Our computational results are consistent with this result, with Per624 being the main triplet quencher in PCP. If we follow first-order TET kinetics for the triplet states in PCP

$$\text{Chl-}a^* \xrightarrow{k_i} \text{Per}_i^* \qquad (19)$$

where Per_i denotes one of the four peridinins in PCP and an asterisk denotes triplet excitation. The kinetics for triplet Chl-*a* can be written as

$$\frac{d[\text{Chl-}a^*]}{dt} = -\sum_i k_i[\text{Chl-}a^*] \qquad (20)$$

and the final triplet population on each peridinin would be proportional to their corresponding TET rates. On the basis of our calculated TET rates, about 85% of BChl-*a* excitation would be quenched by Per624, and for Per622 and Per623, 8 and 7%, respectively. The triplet population transferred to Per621 would be negligible due to its small TET coupling. In a recent TR-EPR work on TET in PCP, several models were suggested to fit the TR-EPR spectra. The ones with a minor component from either Per622 or Per623, and a major component on Per624 fit well to experimental data,[10] and this is very similar to our results. Interestingly, a sequential TET model, in which the Chl-*a* transfers the triplet energy to Per613 (Per623) and then to Per614 (Per624) was proposed, with a prediction that does not fit well to experimental data.[10] According to our results, the

interperidinin TET is not likely to happen either, judged by the small coupling value we obtained (0.06 cm^{-1}, as seen in Table 3).

We note that, similar to LH2, there also is a broad range of T_1 energy that gives rise to TET rate in a similar time scale (Figure 7). Again, it is due to the wide spectral progression in the carotenoid FCWD function. This result shows that using carotenoids in TET as a quenching mechanism is generally robust and applicable. In a recent work,[83] the quenching of triplet Chl-*a* of a series of peridinin analogues were reported. The number of π-conjugated double bonds in the peridinin analogues was varied from 6 to 9, but their TET kinetics with Chl-*a* remain remarkably similar. Therefore, we believe that our modeled T_1 spectra (and the FCWD function) of peridinin is reasonably close to reality.

We have also examined the possibility of forming triplet exciton among the peridinins. Calculated TET couplings between peridinins are listed in Table 3. Coupling values are seen to be slightly larger in Per621−Per622 and Per623−Per624 in comparison to other pairs. However, the triplet excitation energies of peridinins, calculated using TDDFT with PBE functional[78] and 6-31+G* basis, are 0.750, 0.733, 0.668, and 0.812 eV for Per621, Per622, Per623, and Per624, respectively, which gives difference energies of 136 and 1170 cm^{-1} for the two peridinin pairs. These values are too large in comparison with their corresponding TET couplings as listed in Table 3. So we conclude that there is no triplet exciton in the peridinin cluster of PCP.

In present study, we limit our scope to the direct triplet quenching of triplet chlorophylls by carotenoids. However, we cannot rule out other proposed models such as the triplet annihilation in the literature.[20−23] According to our results, the triplet carotenoids can be formed via TET from optically excited Chls or BChls. Triplet annihilation may take place when another triplet (B)Chl is formed.

CONCLUSION

We have calculated the TET electronic coupling and estimated the TET rates for Chls or BChls and carotenoids in photosynthetic light-harvesting complexes, including the LH2 from both *Rs. molischianum* and *Rps. acidophila*, and the PCP from *A. carterae*. We showed that the FSD scheme is a useful tool to study TET for light-harvesting complexes. Our computational results suggest that carotenoids can quench Chl-*a* and BChl-*a* triplets in LH2 and PCP via a direct TET, with the quenching rates in the nanosecond time scales. This result is consistent with several experimental observations. The quenching rates are found to be in the similar order of magnitude in a rather broad range of carotenoid triplet state energy, and this result implies a general and robust TET quenching role for carotenoids in photosynthesis. This result is also consistent with experimental results that showed weak dependence of TET kinetics on the type or the number of π conjugation lengths in the carotenoids and their analogues studied. On the basis of our computational results, triplet excitons among BChl-*a* in LH2, or the peridinins in PCP, are not likely to form.

ASSOCIATED CONTENT

Supporting Information. Supplementary results containing the TDDFT and CIS excitation energies. This material is available free of charge via the Internet at http://pubs.acs.org.

AUTHOR INFORMATION

Corresponding Author
*E-mail: cherri@sinica.edu.tw.

ACKNOWLEDGMENT

We gratefully acknowledge the support from the National Science Council, Republic of China and the Academia Sinica.

REFERENCES

(1) Griffiths, M.; Sistrom, W. R.; Cohen-Bazire, G.; Stanier, R. Y. *Nature* **1955**, *176*, 1211–1214.
(2) Krinsky, N. I. *Philos. Trans. R. Soc., B* **1978**, *284*, 581–590.
(3) Cogdell, R. J.; Frank, H. A. *Biochim. Biophys. Acta* **1987**, *895*, 63–79.
(4) Fraser, N. J.; Hashimoto, H.; Cogdell, R. J. *Photosynth. Res.* **2001**, *70*, 249–256.
(5) Cogdell, R. J.; Hipkins, M. F.; MacDonald, W.; Truscott, T. G. *Biochim. Biophys. Acta* **1981**, *634*, 191–202.
(6) Nagae, H.; Kakitani, T.; Katoh, T.; Mimuro, M. *J. Chem. Phys.* **1993**, *98*, 8012–8023.
(7) Damjanović, A.; Ritz, T.; Schulten, K. *Phys. Rev. E* **1999**, *59*, 3293–3311.
(8) Damjanović, A.; Ritz, T.; Schulten, K. *Biophys. J.* **2000**, *79*, 1695–1705.
(9) Bittl, R.; Schlodder, E.; Geisenheimer, I.; Lubitz, W.; Cogdell, R. J. *J. Phys. Chem. B* **2001**, *105*, 5525–5535.
(10) Di Valentin, M.; Ceola, S.; Salvadori, E.; Agostini, G.; Carbonera, D. *Biochim. Biophys. Acta* **2008**, *1777*, 186–195.
(11) Dexter, D. L. *J. Chem. Phys.* **1953**, *21*, 836–850.
(12) Harcourt, R. D.; Scholes, G. D.; Ghiggino, K. P. *J. Chem. Phys.* **1994**, *101*, 10521–10525.
(13) Scholes, G. D.; Harcourt, R. D.; Ghiggino, K. P. *J. Chem. Phys.* **1995**, *102*, 9574–9581.
(14) Harcourt, R. D.; Ghiggino, K. P.; Scholes, G. D.; Speiser, S. *J. Chem. Phys.* **1996**, *105*, 1897–1901.
(15) You, Z.-Q.; Hsu, C.-P. *J. Chem. Phys.* **2010**, *133*, 074105.
(16) Curutchet, C.; Voityuk, A. A. *Angew. Chem., Int. Ed.* **2011**, *50*, 1820–1822.
(17) Cogdell, R. J.; Howard, T. D.; Bittl, R.; Schlodder, E.; Geisenheimer, I.; Lubitz, W. *Philos. Trans. R. Soc., B* **2000**, *355*, 1345–1349.
(18) Bautista, J. A.; Hiller, R. G.; Sharples, F. P.; Gosztola, D.; Wasielewski, M.; Frank, H. A. *J. Phys. Chem. A* **1999**, *103*, 2267–2273.
(19) Di Valentin, M.; Ceola, S.; Agostini, G.; Giacometti, G. M.; Angerhofer, A.; Crescenzi, O.; Barone, V.; Carbonera, D. *Biochim. Biophys. Acta* **2008**, *1777*, 295–307.
(20) Limantara, L.; Fujii, R.; Zhang, J.-P.; Kakuno, T.; Hara, H.; Kawamori, A.; Yagura, T.; Cogdell, R. J.; Koyama, Y. *Biochemistry* **1998**, *37*, 17469–17486.
(21) Rondonuwu, F. S.; Taguchi, T.; Fujii, R.; Yokoyama, K.; Koyama, Y.; Watanabe, Y. *Chem. Phys. Lett.* **2004**, *384*, 364–371.
(22) Alexandre, M. T. A.; Lührs, D. C.; van Stokkum, I. H. M.; Hiller, R.; Groot, M.-L.; Kennis, J. T. M.; van Grondelle, R. *Biophys. J.* **2007**, *93*, 2118–2128.
(23) Bonetti, C.; Alexandre, M. T. A.; Hiller, R. G.; Kennis, J. T. M.; van Grondelle, R. *Chem. Phys.* **2009**, *357*, 63–69.
(24) Monger, T. G.; Cogdell, R. J.; Parson, W. W. *Biochim. Biophys. Acta* **1976**, *449*, 136–153.
(25) Zimmermann, J.; Linden, P. A.; Vaswani, H. M.; Hiller, R. G.; Fleming, G. R. *J. Phys. Chem. B* **2002**, *106*, 9418–9423.
(26) Bautista, J. A.; Connors, R. E.; Raju, B. B.; Hiller, R. G.; Sharples, F. P.; Gosztola, D.; Wasielewski, M. R.; Frank, H. A. *J. Phys. Chem. B* **1999**, *103*, 8751–8758.

(27) Frank, H. A.; Bautista, J. A.; Josue, J.; Pendon, Z.; Hiller, R. G.; Sharples, F. P.; Gosztola, D.; Wasielewski, M. R. *J. Phys. Chem. B* **2000**, *104*, 4569–4577.
(28) Vaswani, H. M.; Hsu, C.-P.; Head-Gordon, M.; Fleming, G. R. *J. Phys. Chem. B* **2003**, *107*, 7940–7946.
(29) Di Valentin, M.; Ceola, S.; Salvadori, E.; Agostini, G.; Giacometti, G. M.; Carbonera, D. *Biochim. Biophys. Acta* **2008**, *1777*, 1355–1363.
(30) Di Valentin, M.; Salvadori, E.; Ceola, S.; Carbonera, D. *Appl. Magn. Reson.* **2010**, *37*, 191–205.
(31) Hofmann, E.; Wrench, P. M.; Sharples, F. P.; Hiller, R. G.; Welte, W.; Diederichs, K. *Science* **1996**, *272*, 1788–1791.
(32) Koepke, J.; Hu, X.; Muenke, C.; Schulten, K.; Michel, H. *Structure* **1996**, *4*, 581–597.
(33) McDermott, G.; Prince, S. M.; Freer, A. A.; Hawthornthwaite-Lawless, A. M.; Papiz, M. Z.; Cogdell, R. J.; Isaacs, N. W. *Nature* **1995**, *374*, 517–521.
(34) Fleming, G. R.; van Grondelle, R. *Curr. Opin. Struct. Biol.* **1997**, *7*, 738–748.
(35) Cheng, Y. C.; Silbey, R. J. *Phys. Rev. Lett.* **2006**, *96*, 028103.
(36) Prince, S. M.; Papiz, M. Z.; Freer, A. A.; McDermott, G.; Hawthornthwaite-Lawless, A. M.; Cogdell, R. J.; Isaacs, N. W. *J. Mol. Biol.* **1997**, *268*, 412–423.
(37) Papiz, M. Z.; Prince, S. M.; Howard, T.; Cogdell, R. J.; Isaacs, N. W. *J. Mol. Biol.* **2003**, *326*, 1523–1538.
(38) Carbonera, D.; Giacometti, G.; Segre, U.; Angerhofer, A.; Gross, U. *J. Phys. Chem. B* **1999**, *103*, 6357–6362.
(39) Dirac, P. A. M. *Proc. R. Soc. London, Ser. A* **1927**, *114*, 243–265.
(40) Lin, S. H. *Proc. R. Soc. London, Ser. A* **1973**, *335*, 51–66.
(41) Förster, T. *Ann. Phys. (Leipzig)* **1948**, *2*, 55–75.
(42) Lin, S. H. *Theor. Chim. Acta* **1968**, *10*, 301–310.
(43) Lax, M. *J. Chem. Phys.* **1952**, *20*, 1752–1760.
(44) Yersin, H.; Otto, H.; Zink, J. I.; Gliemann, G. *J. Am. Chem. Soc.* **1980**, *102*, 951–955.
(45) Caspar, J. V.; Westmoreland, T. D.; Allen, G. H.; Bradley, P. G.; Meyer, T. J.; Woodruff, W. H. *J. Am. Chem. Soc.* **1984**, *106* 3492–3500.
(46) Huang, K.; Rhys, A. *Proc. R. Soc. London, Ser. A* **1950**, *204*, 406–423.
(47) Murtaza, Z.; Zipp, A. P.; Worl, L. A.; Graff, D.; Jones, W. E., Jr.; Bates, W. D.; Meyer, T. J. *J. Am. Chem. Soc.* **1991**, *113*, 5113–5114.
(48) Murtaza, Z.; Graff, D. K.; Zipp, A. P.; Worl, L. A.; Jones, W. E., Jr.; Bates, W. D.; Meyer, T. J. *J. Phys. Chem.* **1994**, *98*, 10504–10513.
(49) Liang, Y. Y.; Baba, A. I.; Kim, W. Y.; Atherton, S. J.; Schmehl, R. H. *J. Phys. Chem.* **1996**, *100*, 18408–18414.
(50) Christensen, R. L. In *The Photochemistry of Carotenoids*; Frank, H. A., Young, A. J., Nritton, G., Cogdell, R. J., Eds.; Kluwer Academic Publishers: Dordrecht, 1999; pp 137−159.
(51) Hudson, B. S.; Kohler, B. E.; Schulten, K. In *Excited States*; Lim, E. C., Ed.; Academic Press: New York, 1982; Vol. 6; pp 1−95.
(52) Georgakopoulou, S.; van Grondelle, R.; van der Zwan, G. *Biophys. J.* **2004**, *87*, 3010–3022.
(53) Billsten, H. H.; Herek, J. L.; Garcia-Asua, G.; Hashøj, L.; Polívka, T.; Hunter, C. N.; Sundström, V. *Biochemistry* **2002**, *41*, 4127–4136.
(54) Polívka, T.; Zigmantas, D.; Herek, J. L.; He, Z.; Pascher, T.; Pullerits, T.; Cogdell, R. J.; Frank, H. A.; Sundström, V. *J. Phys. Chem. B* **2002**, *106*, 11016–11025.
(55) Neverov, K. V.; Krasnovsky, A. A., Jr. *Biofizika* **2004**, *49*, 493–498.
(56) Kleima, F. J.; Wendling, M.; Hofmann, E.; Peterman, E. J. G.; van Grondelle, R.; van Amerongen, H. *Biochemistry* **2000**, *39*, 5184–5195.
(57) Polívka, T.; Hiller, R. G.; Frank, H. A. *Arch. Biochem. Biophys.* **2007**, *458*, 111–120.
(58) Cave, R. J.; Newton, M. D. *Chem. Phys. Lett.* **1996**, *249*, 15–19.
(59) Voityuk, A. A.; Rösch, N. *J. Chem. Phys.* **2002**, *117*, 5607–5616.
(60) Hsu, C.-P.; You, Z.-Q.; Chen, H.-C. *J. Phys. Chem. C* **2008**, *112*, 1204–1212.
(61) Subotnik, J. E.; Vura-Weis, J.; Sodt, A. J.; Ratner, M. A. *J. Phys. Chem. A* **2010**, *114*, 8665–8675.
(62) Becke, A. D. *Phys. Rev. A* **1988**, *38*, 3098–3100.
(63) Lee, C.; Yang, W.; Parr, R. G. *Phys. Rev. B* **1988**, *37*, 785–789.
(64) Stephens, P. J.; Devlin, F. J.; Chabalowski, C. F.; Frisch, M. J. *J. Phys. Chem.* **1994**, *98*, 11623–11627.
(65) Mao, L.; Wang, Y.; Hu, X. *J. Phys. Chem. B* **2003**, *107*, 3963–3971.
(66) Shao, Y.; et al. *Phys. Chem. Chem. Phys.* **2006**, *8*, 3172–3191.
(67) *MATLAB, version 7.9.0*; The MathWorks, Inc.: Natick, MA, 2009.
(68) You, Z.-Q.; Hsu, C.-P.; Fleming, G. R. *J. Chem. Phys.* **2006**, *124*, 044506.
(69) Schweitzer, C.; Schmidt, R. *Chem. Rev.* **2003**, *103*, 1685–1758.
(70) Farhoosh, R.; Chynwat, V.; Gebhard, R.; Lugtenburg, J.; Frank, H. *Photosynth. Res.* **1994**, *42*, 157–166.
(71) Jacquemin, D.; Perpète, E. A.; Ciofini, I.; Adamo, C. *J. Chem. Theory Comput.* **2010**, *6*, 1532–1537.
(72) Silva-Junior, M. R.; Schreiber, M.; Sauer, S. P. A.; Thiel, W. *J. Chem. Phys.* **2008**, *129*, 104103.
(73) Grimme, S.; Neese, F. *J. Chem. Phys.* **2007**, *127*, 154116.
(74) Cui, G.; Yang, W. *Mol. Phys.* **2010**, *108*, 2745–2750.
(75) Nguyen, K. A.; Kennel, J.; Pachter, R. *J. Chem. Phys.* **2002**, *117*, 7128–7136.
(76) Sundholm, D. *Chem. Phys. Lett.* **2000**, *317*, 392–399.
(77) Sundholm, D. *Phys. Chem. Chem. Phys.* **2000**, *2*, 2275–2281.
(78) Perdew, J. P.; Burke, K.; Ernzerhof, M. *Phys. Rev. Lett.* **1996**, *77*, 3865–3868.
(79) Jimenez, R.; Dikshit, S. N.; Bradforth, S. E.; Fleming, G. R. *J. Phys. Chem.* **1996**, *100*, 6825–6834.
(80) Kennis, J. T. M.; Streltsov, A. M.; Permentier, H.; Aartsma, T. J.; Amesz, J. *J. Phys. Chem. B* **1997**, *101*, 8369–8374.
(81) Sundström, V.; Pullerits, T.; van Grondelle, R. *J. Phys. Chem. B* **1999**, *103*, 2327–2346.
(82) Trautman, J. K.; Shreve, A. P.; Violette, C. A.; Frank, H. A.; Owens, T. G.; Albrecht, A. C. *Proc. Natl. Acad. Sci. U.S.A.* **1990**, *87*, 215–219.
(83) Kaligotla, S.; Doyle, S.; Niedzwiedzki, D. M.; Hasegawa, S.; Kajikawa, T.; Katsumura, S.; Frank, H. *Photosynth. Res.* **2010**, *103*, 167–174.